

## Supporting Information

### A Multiscale Flexible Pressure Sensor Based on Nanovesicle-Like Hollow Microspheres for Micro-Vibration Detection in Non-Contact Mode

Tie Li,<sup>1</sup> Lili Li,<sup>1</sup> Yuanyuan Bai,<sup>1</sup> Yudong Cao,<sup>1</sup> Qifeng Lu,<sup>1</sup> Yue Li,<sup>1</sup> Gengzhao Xu<sup>2</sup> and Ting Zhang<sup>1\*</sup>  
1: *i*-Lab and 2: Platform for Characterization & Test, Suzhou Institute of Nano-Tech and Nano-Bionics, Chinese Academy of Sciences, 398 Ruoshui Road, Suzhou, 215123, P. R. China  
\* corresponding author: Ting Zhang: E-mail: [tzhang2009@sinano.ac.cn](mailto:tzhang2009@sinano.ac.cn)

#### Table of Contents

**S1:** Preparation of mono-dispersed SiO<sub>2</sub> spheres

**S2:** Preparation of Microstructural Flexible Substrates

S3. The Reason Why a PDMS-PE Composite Was Used As Substrate

**Fig. S1.** The damaged condition of flexible sensor directly pasted on the surface of analyte in rigorous situations.

**Fig. S2:** The Zeta potential of reaction conditions controlled through the participated ethanol volume and HCl concentration, respectively.

**Fig. S3:** The as-prepared SiO<sub>2</sub>/PPy core-shell composites by adjusting the concentration of initiator.

**Fig. S4.** The response property of sensor prepared by pure PPy nanoparticles without spherical structure.

**Fig. S5.** The dynamic response of the flexible sensor by adjusting the volume of Py monomer at 25 μL, 50 μL, 100 μL and 150 μL under the same 0.1 g initiator, respectively.

**Fig. S6.** The SEM images of sensing materials after 2500 cycling tests and the enlarged morphology of hollow microspheres.

**Fig. S7.** The micro pressure induced displacement from the contact of pyramid structure by the mode of (a) point-to-point and (b) side-to-side.

**Fig. S8:** The morphology and structure of PPy hollow microspheres with simplex full-shell structure.

**Fig. S9.** The controlled response tests for the water flow and inelastic collision under without PPy microspheres, pramid microstructure and Ag NWs.

**Fig. S10:** The repeatability tests of the sensor to the micro-vibration signals induced by the airflow.

**Fig. S11:** The existed full-contacting pressure-controlled hand gesture recognition or human-machine interaction.

### **S1. Preparation of mono-dispersed SiO<sub>2</sub> spheres:**

Briefly, NH<sub>3</sub>·H<sub>2</sub>O (7.5 mL) was added into a solution containing ethanol (120 mL) and deionized water (18 mL). Separately, tetraethyl orthosilicate (TEOS, 3.8 mL) was mixed with ethanol (10 mL). After these two solutions were rapidly mixed under vigorous stirring, the mixture was kept stirring for 12 h to yield uniform mono-dispersed silicon dioxide (SiO<sub>2</sub>) spheres. The resulting mono-dispersed SiO<sub>2</sub> spheres were separated by centrifugation at 8000 rpm for 10 min and washed several times with ethanol and water.

### **S2. Preparation of Microstructural Flexible Substrates:**

Silicon (Si) wafers ((100), 0.5 mm thick, 4 inch) with 300 nm SiO<sub>2</sub> layers was chosen as origin mold. Photolithography (AZ5214) was inlaid with grid pattern on origin Si mold to produce pyramid microstructures. The exposed SiO<sub>2</sub> patterns were etched by reactive ion etching. The Si substrate was put into a wet etching solution (40 wt.% KOH in deionized water) at 80 °C for 10 min to obtain the uniform recessed pyramid patterns (10 μm × 10 μm × 7 μm) with a 10 μm interval.

The as-obtained patterned Si mold with recessed pyramid microstructures was soaked in the mold release-agent of chlorotrimethylsilane. And then, a semi-solidified PDMS film with 20 μm thick was formed on the surface of this microstructural Si mold by spin-coating (3000 rpm, 30 s) and heated at 70 °C for 5 min. Meanwhile, an ultraviolet treated polyethylene (PE) film (10 μm thick) was laminated on top of the semi-solidified PDMS that used as an encapsulation layer. Finally, PDMS-PE composite film with pyramid microstructures was obtained by solidification treatment process at 70 °C for 2 h and subsequently employed as flexible substrates.

### **S3. The Reason Why a PDMS-PE Composite Was Used As Substrate:**

As well known, Polydimethylsiloxane (PDMS) acted as a soft polymer has been widely adopted as a substrate material for manufacturing flexible electronic devices owing to its elasticity and stretchability. <sup>[E1]</sup> It has also been regarded as a suitable material for fabrication and replica of microstructure to reinforce performance and sensitivity of device. <sup>[E2]</sup> But the stability and repeatability of the device has some difficulty to achieve due to its lower mechanical property and smaller Young's modulus. <sup>[E3]</sup> Therefore, a 10  $\mu\text{m}$  thick polyethylene (PE) film was used to reinforce tenacity and mechanical property of PDMS by ultraviolet (UV) treated for 5 min. The adhesive of interface was fastness with crosslink of chemical bond which introduced by Fourier transform infrared spectroscopy (FTIR), and the modulus of the fabricated PDMS-PE bilayer could be tuned in the range of 2-40 MPa, which has been proved by our previous research. <sup>[E4]</sup> Hence, here the PDMS-PE composite film was chosen as flexible substrate, which possesses a suitable modulus for high sensitivity of pressure sensor.

[E1]: S. C. L. Fischer, O. Levy, E. Kroner, R. Hensel, J. M. Karp, and E. Arzt, *J. Mech. Behav. Biomed. Mater.*, 2016, **61**, 87-95.

[E2]: Y. N. Xia, and G. M. Whitesides, *Angew. Chem. Int. Ed.*, 1998, **37**, 550.

[E3]: I. D. Johnston, D. K. McCluskey, C. K. L. Tan, and M. C. Tracey, *J. Micromech. Microeng.*, 2014, **24**, 035017.

[E4]: Y. Gu, X. W. Wang, W. Gu, J. Y. Wu, T. Li, and T. Zhang, *Nano Res.*, 2017, **10**, 2683.  
**(Our previous works)**

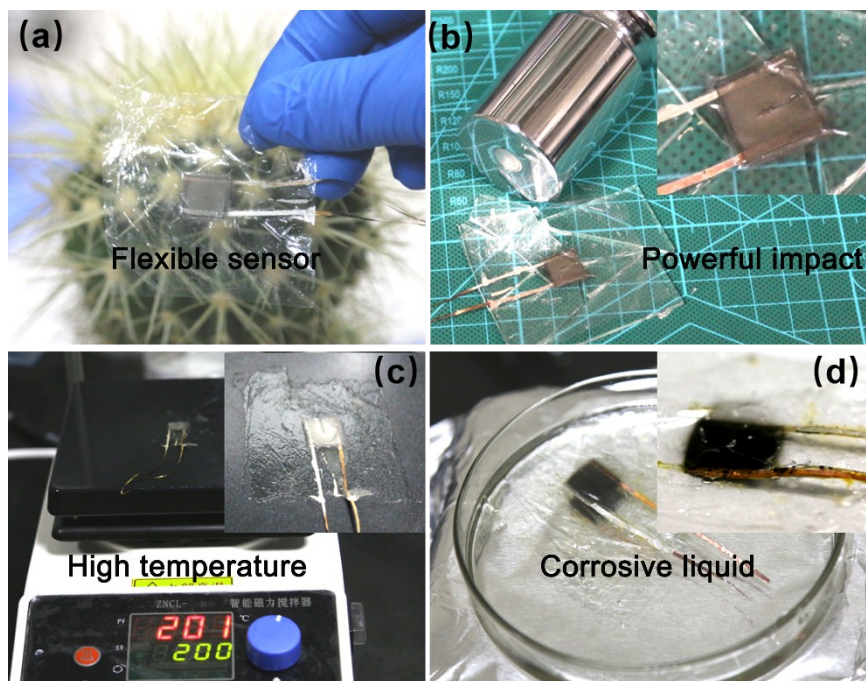


**Fig. S1.** The damaged conditions of (a) flexible sensor directly pasted on the surface of analyte in rigorous situations: (b) powerful impact, (c) high temperature surface, and (d) corrosive liquid environment, respectively.

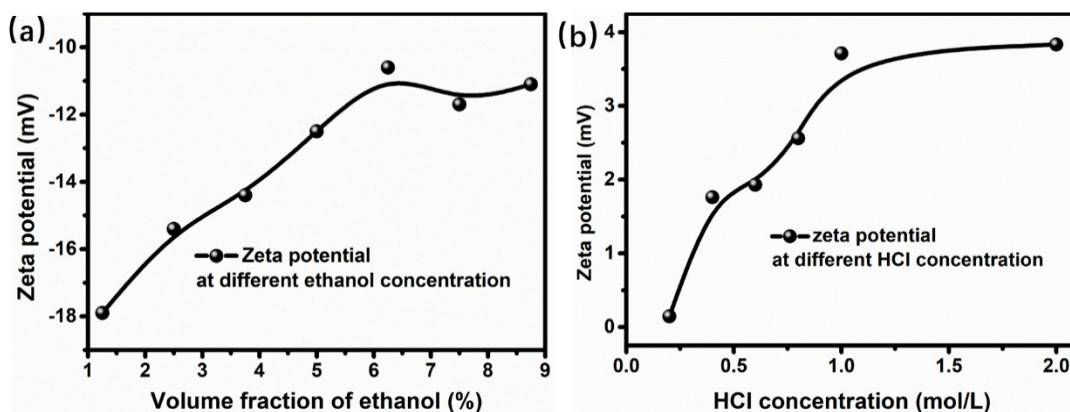


**Fig. S2.** The Zeta potential of reaction conditions controlled through the participated ethanol volume (a) and HCl concentration (b), respectively.

The surface energy, which relies on the Zeta potential of reaction conditions, can be controlled through the participated ethanol volume and HCl concentration. As shown in Fig. S1, the results of Zeta potential all shows the increase tendency along with the addition of ethanol and HCl, indicating the reaction conditions change of solution and further influence the surface energy match ( $\gamma$ ) of the multi-phase interface ( $\Delta G_s$ ). The reason why these occurred can be concluded as: Well known the pyrrole monomer contains a pair of lone pairs of electrons on the nitrogen atom which electron effect is greater than electron absorption. Complementary,  $\text{SiO}_2$  suspension showed electro-negativity by zeta potential. Hence, the self-assembly process of the PPy- $\text{SiO}_2$  microspheres is progressed according to two competitive interactions, one is the hydrogen bonding attraction between the pyrrolic nitrogen (N-H) group of Py and the hydroxyl (-OH) group of  $\text{SiO}_2$  nanoparticles, and the other is the electrostatic repulsion between the protonated Py monomer and -OH group of  $\text{SiO}_2$  nanoparticles. Under the low volume and concentration of ethanol and HCl respectively, the electronegativity difference of Zeta potential is the maximum, which possesses the supreme hydrogen bonding attraction, resulting the full core-shell morphology. And at the top points of volume and concentration, the electronegativity difference is the minimum, which causes the non-continuously assembling tendency. Between above two mode, the tends is to form the layer assembly core-shell structure at early and then produce the partially engulfing island structure, resulting the vesicles-like microsphere structure. Hence, in this study, the middle parameters 4-5 % ethanol (10 mL) and 1 mol/L HCl (50 mL of 5 M HCl added into 200 mL) in 250 mL was chosen as the experiment conditions.

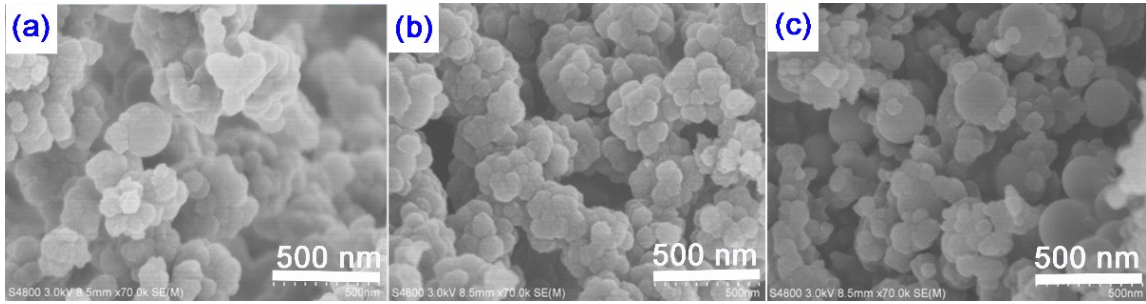


**Fig. S3.** The as-prepared SiO<sub>2</sub>/PPy core-shell composites by adjusting the concentration of initiator at (a) 0.05 g, (b) 0.1 g and (c) 0.15 g, respectively.

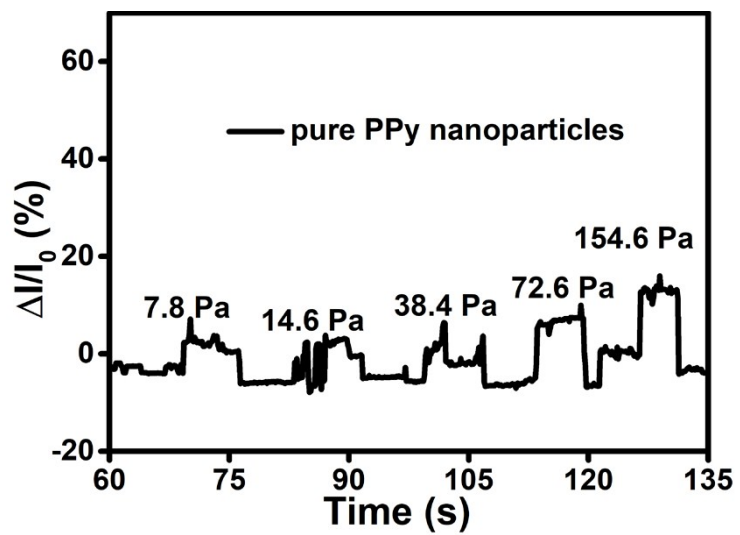


**Fig. S4.** The response property of sensor prepared by pure PPy nanoparticles without spherical structure.

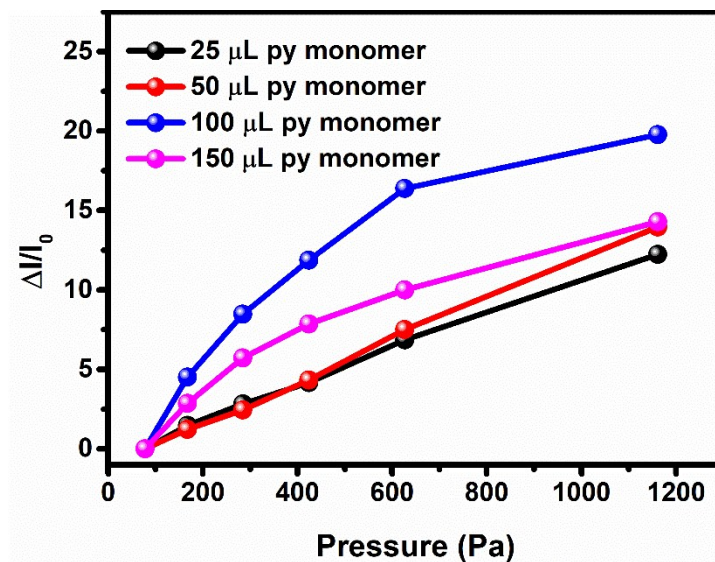


**Fig. S5.** The dynamic response of the flexible sensor by adjusting the volume of Py monomer at 25  $\mu\text{L}$ , 50  $\mu\text{L}$ , 100  $\mu\text{L}$  and 150  $\mu\text{L}$  under the same 0.1 g initiator, respectively.

From the Fig. S2, it can be clearly seen that only 0.1 g of initiator can obtain the unbroken PPy-  $\text{SiO}_2$  structure, here it was chosen as the best amount of initiator. Then, from the Fig. 2., it can be obviously seen that the products prepared by 100  $\mu\text{L}$  of Py monomer under 0.1 g of initiator reveal the optimal morphology and structure. Lastly, through the optimal dynamic response in Fig. S3, the best reaction parameters to synthesize the designed microspheres are chosen as 100  $\mu\text{L}$  of Py monomer and 0.1 g of initiator, which was caused by the optimal morphology and structure in Fig. 2.



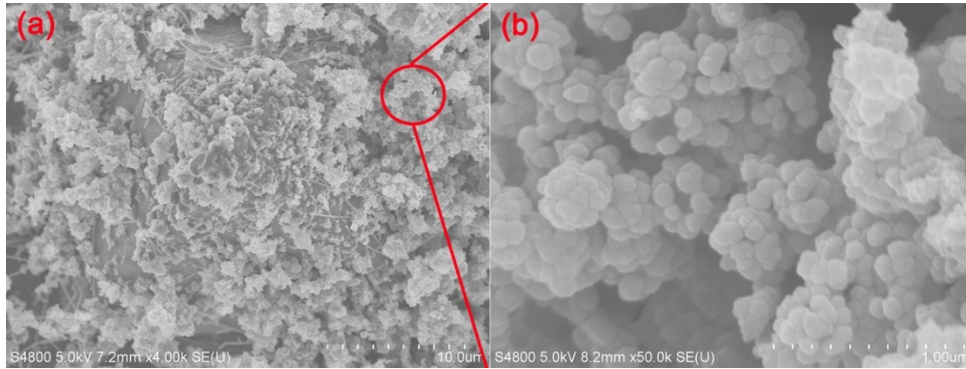


**Fig. S6.** The SEM images of sensing materials after 2500 cycling tests (a) and the enlarged morphology of hollow microspheres (b).

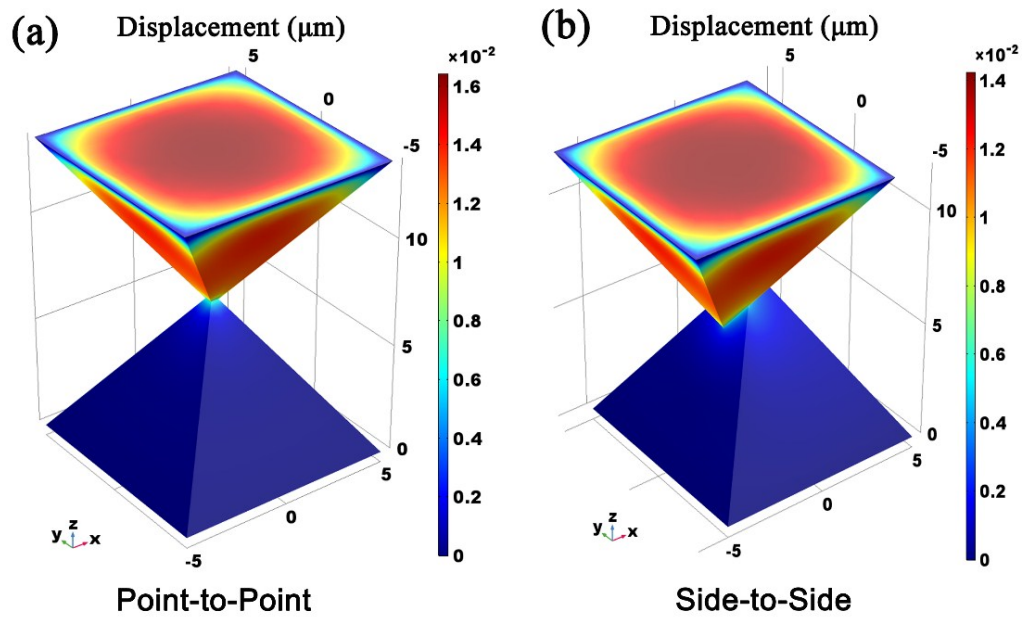


**Fig. S7.** The micro pressure induced displacement from the contact of pyramid structure by the mode of (a) point-to-point and (b) side-to-side.

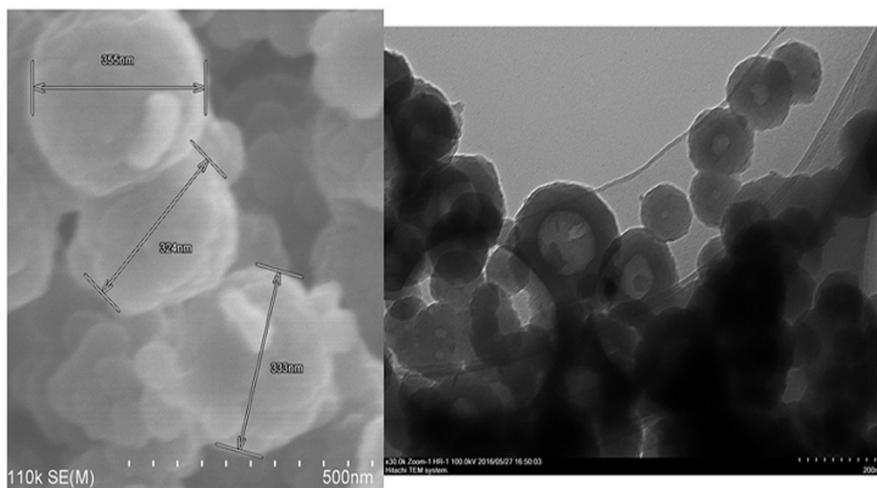


**Fig. S8.** The morphology and structure of PPy hollow microspheres with simplex full-shell structure according to the Frank-Vander Merwe model ( $\Delta G_s > 0$ )

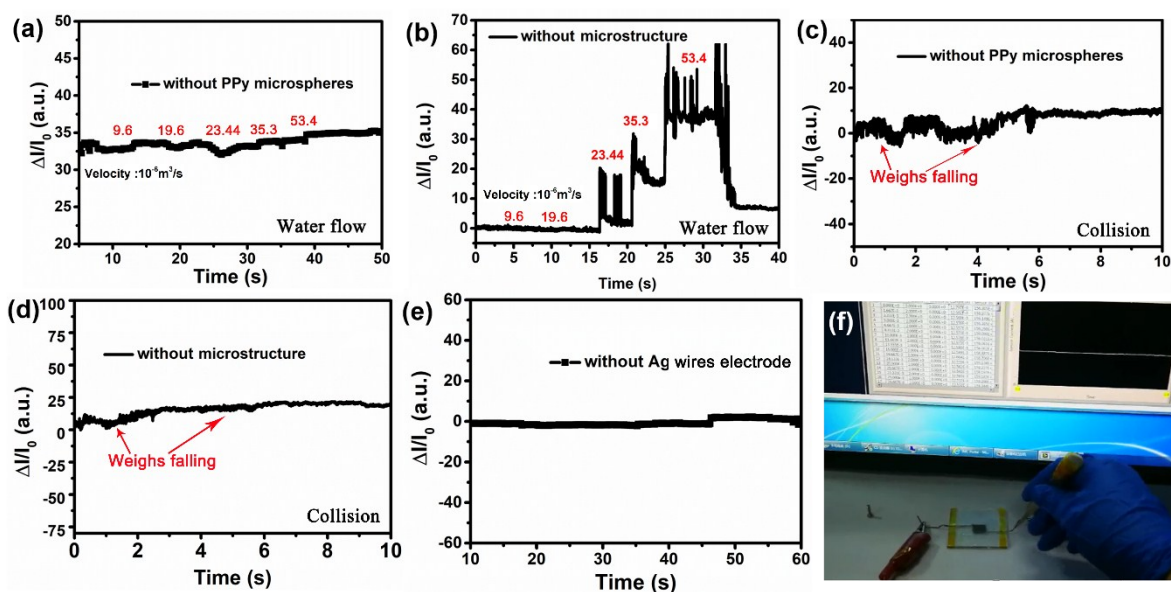


**Fig. S9.** The controlled response tests for (a-b) the water flow and (c-d) inelastic collision when executed without PPy microspheres and pyramid microstructures under the same test conditions. And it can be seen that the Ag wires electrode movement cannot produce the unwanted signals (e-f).

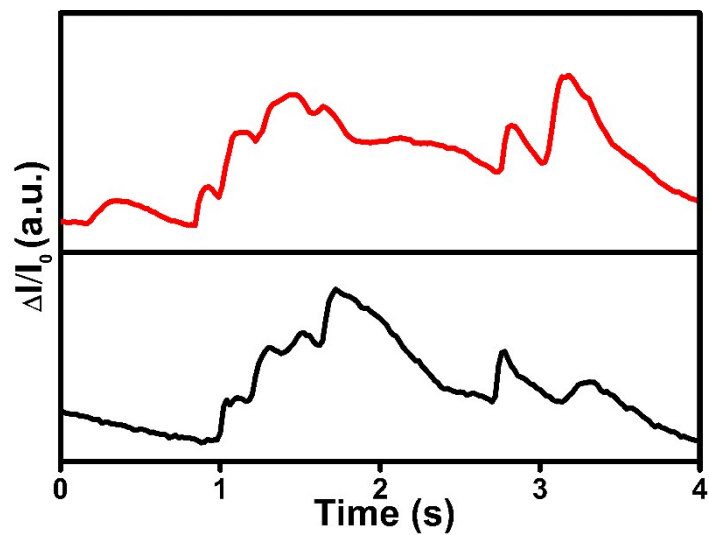


**Fig. S10.** The repeatability tests of the sensor to the micro-vibration signals induced by the airflow.



**Fig. S11.** The existed full-contacting pressure-controlled hand gesture recognition or human-machine interaction.